

IDENTIFICATION OF DYNAMICAL SYSTEMS WITH TIME-VARYING DISTURBANCES AND FRACTIONAL ERRORS-IN-VARIABLES. APPLICATION EXAMPLE TO A DRONE MODEL

Dmitriy Ivanov

Department of Information Systems Security
Samara National Research University
Department of Digital Technologies,
Samara State University of Transport
Samara, Russia
d.ivanov@samgups.ru

Aleksandr Zhdanov

Department of Applied Mathematics and Computer Science,
Samara State Technical University
Samara, Russia
zhdanovaleksan@yandex.ru

Ilya Sandler

Department of Automation and control in technical systems
Samara State Technical University
Department of Digital Technologies,
Samara State University of Transport
Samara, Russia
i.sandler@samgups.ru

Article history:

Received 13.05.2024, Accepted 17.06.2024

Abstract

The article discusses the problem of identification of motion model parameters for UAV with nonstationary disturbances and fractional errors-in-variables. A total least squares (TLS)-based identification method for the solution of generalized instrumental variables of the estimator is proposed. The proposed method is compared with least squares (LS) and extended instrumental variables (EIV). To increase numerical stability, all identification methods are implemented based augmented systems of equations. The simulation results showed the advantage of the presented method.

Key words

UAV, quadrotor, identification, estimation, errors-in-variables, total least squares, instrumental variables, fractional noise.

1 Introduction

In several recent years, there has been a great boom on many kinds of the unmanned aerial vehicles (UAVs), especially vertical take-off and landing platforms with multirotor actuators. A large number of articles have

been devoted to identifying the dynamics models of UAVs. Linear models in the time domain were considered in article [Gremillion and Humbert, 2010]. The Kalman filter for identifying flight dynamics was used in article [Abas et al., 2011], subspace identification methods are considered in article [Bergamasco, 2014]. The use of ARX, ARMAX, BJ, ARIMAX models is described in articles [Belge, 2020; Khaled and Boumehraz, 2022; Suliman et al., 2023]. Identification of dynamics in the frequency domain is described in articles [Wei et al., 2014; Wei et al., 2017; Huang et al., 2021; Yang et al., 2021]. A comparison of methods in the time and frequency domains is made in article [Wu and Lovera., 2019]. Identification algorithms for under unknown-but bounded disturbance are discussed in the articles [Amelin, 2012; Amelin and Maltsev, 2021; Ivanov et al., 2023]. The identification of nonlinear models is considered in article [Avdeev et al., 2021]. A review of various UAV model identification methods is presented [Elgmili et al., 2019]. Most methods assume that identification occurs under the condition that the noise is stationary and represents ARMA processes. However, the measurement noise of the sensors and constantly changing flight conditions require the develop-

ment of methods that allow identification in more complex conditions. The article proposes an identification of vertical movement model UAV with nonstationary disturbances and fractional errors-in-variables.

2 Problem Statement and the Theoretical Framework

There are a large number of publications in the literature that provide equations for the dynamics of a quadcopter, for example in [Castillo et al., 2005; Janusz and Szafranski, 2013].

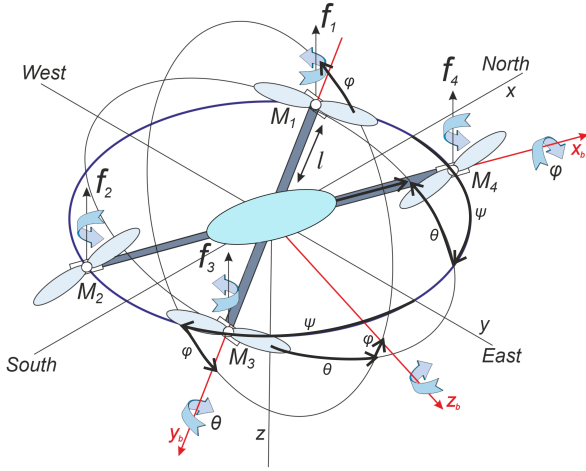


Figure 1. A typical model of a quadrotor helicopter.

This article uses a dynamics model derived from the Euler–Lagrange equations under the following assumptions:

A1. The quadcopter design is rigid, symmetrical about the vertical axis.

A2. The center of mass lies at the origin of the associated coordinate system.

A3. The bending of the structure can be neglected.

$$\begin{cases} I_x \ddot{\varphi} = (I_y - I_z) \dot{\theta} \dot{\psi} + T_\varphi(t) \\ I_y \ddot{\theta} = (I_z - I_x) \dot{\psi} \dot{\varphi} + T_\theta(t) \\ I_z \ddot{\psi} = (I_x - I_y) \dot{\theta} \dot{\varphi} + T_\psi(t) \\ m \ddot{x} = (\sin(\psi) \sin(\varphi) + \cos(\psi) \sin(\theta) \cos(\varphi)) f(t) \\ m \ddot{y} = (\sin(\psi) \sin(\theta) \cos(\varphi) - \cos(\psi) \sin(\varphi)) f(t) \\ m \ddot{z} = (\cos(\theta) \cos(\varphi)) f(t) - g \end{cases} \quad (1)$$

where

θ, ψ, φ are the Euler angles;

x, y, z is the position of the centre of quadrotor mass with respect to a fixed reference frame;

I_x, I_y, I_z are inertia moments;

$T_\theta(t)$, are torques consist of the difference in the action of the thrust forces for each pair and the gyroscopic effect;

m is platform's mass;

g is Earth's gravity acceleration,

$f(t)$ is total thrust coming from the rotors.

The total thrust is given as

$$f(t) = f_1(t) + f_2(t) + f_3(t) + f_4(t), \quad (2)$$

where $f_i(t), i = 1 \dots 4$ are forces applied by rotating propellers.

These forces depend on the rotation speed of the rotors and the behavior of the air flow near the quadcopter. This paper considers the movement of a quadcopter in height $z(t)$ under the assumption that it is oriented horizontally. Therefore, the angles θ, φ in (1) are considered zero, and the yaw angle is not significant. From this we obtain the following model of isolated vertical motion:

$$m \ddot{z}(t) = f(t) - mg. \quad (3)$$

Let us refine model (3), taking into account the interaction between the rotating blades and the surrounding air. This interaction is complex [Janusz and Szafranski, 2013; Amelin et al., 2015; Amelin et al., 2019]. Based on [Janusz and Szafranski, 2013], we further suggest that this interaction in vertical motion can be represented by a viscous friction model. Then instead of (3) we use a model of the form

$$\ddot{z}(t) + K \dot{z}(t) = K_\omega \sum_{i=1}^4 \omega_i(t) - mg, \quad (4)$$

where $\omega_i(t), i = 1 \dots 4$ are angular speeds of rotation of propellers, is viscous friction coefficient, K_ω is propeller efficiency coefficient.

Taking into account the assumption that the quadcopter is flying without tilting, we assume that

$$\omega_1(t) = \omega_2(t) = \omega_3(t) = \omega_4(t).$$

Neglecting the dynamics of electric motors, we obtain the following model of the dynamics of vertical motion:

$$\ddot{z}(t) + K \dot{z}(t) = K_u u(t) - g, \quad (5)$$

where K, K_u are coefficients of the model;

$\sum_{i=1}^4 u_i(t)$ is height control signal (sum of voltages $u_i(t)$ applied to the motors).

The values of K, K_u depend on many factors and are difficult to calculate directly. To find their values, we use identification based on processing experimental data. The equation (5) in matrix form is described as

$$\ddot{z}(t) - g = \varphi(t) \theta, \quad (6)$$

where

$$\varphi(t) = (-\dot{z}(t) \ u(t)),$$

$$\theta = (K \ K_u)^T.$$

3 Error in Equation and Least Squares (LS)

Let us add to equation (6) the error in equation

$$\ddot{z}(t) - g = \varphi(t)\theta + \zeta(t). \quad (7)$$

Equation (7) in discrete time is described as

$$\ddot{z}(t_k) - g = \varphi(t_k)\theta + \zeta(t_k). \quad (8)$$

The least squares estimate of the vector can be found as [Amelin et al., 2015; Amelin et al., 2019]

$$\hat{\theta}_{LS} = (\Phi^T \Phi)^{-1} \Phi^T (\ddot{Z} - g), \quad (9)$$

where

$$\ddot{Z} = \begin{pmatrix} \ddot{z}(t_1) - g \\ \vdots \\ \ddot{z}(t_N) - g \end{pmatrix}, \Phi = \begin{pmatrix} \varphi(t_1) \\ \vdots \\ \varphi(t_N) \end{pmatrix}.$$

The system of linear equations (9) can be solved using the Cholesky decomposition or using the augmented system of equations [Björck, 1967]:

$$\begin{pmatrix} K_{LS} E_N & \Phi \\ \Phi^T & 0 \end{pmatrix} \begin{pmatrix} K_{LS}^{-1} \varepsilon \\ \theta \end{pmatrix} = \begin{pmatrix} \ddot{Z} - g \\ 0 \end{pmatrix}, \quad (10)$$

where $K_{LS} = \frac{\sigma_{\min}}{\sqrt{2}}$, σ_{\min} is minimal singular number of matrix Φ .

4 Errors-in-Variables and total least squares (TLS)

We will assume that the model of input and output signals is observed with errors

$$\begin{aligned} \tilde{z}(t_k) &= \dot{z}(t_k) + \dot{\xi}(t_k), \tilde{\ddot{z}}(t_k) = \ddot{z}(t_k) + \ddot{\xi}(t_k), \\ \tilde{u}(t_k) &= u(t_k) + \xi_u(t_k). \end{aligned} \quad (11)$$

For noisy measurement, equation (6) is described as

$$\tilde{\ddot{z}}(t) - g = \tilde{\varphi}(t)\theta + \varepsilon(t), \quad (12)$$

where

$$\begin{aligned} \varepsilon(t) &= \ddot{\xi}(t) + \varphi_{\xi\zeta}(t)\theta, \\ \varphi_{\xi\zeta}(t) &= \tilde{\varphi}(t) - \varphi(t). \end{aligned}$$

Let us make the following assumption about noise:

A4. The noise sequences $\{\ddot{\xi}(t_k)\}$, $\{\dot{\xi}(t_k)\}$, $\{\zeta(t_k)\}$ are independent sequences with

$$\begin{aligned} E(\ddot{\xi}(t_k)) &= 0, E(\dot{\xi}(t_k)) = 0, E(\zeta(t_k)) = 0, \\ E(\ddot{\xi}^2(t_k)) &= \sigma_{\ddot{\xi}}^2, E(\dot{\xi}^2(t_k)) = \sigma_{\dot{\xi}}^2, E(\zeta^2(t_k)) = \sigma_{\zeta}^2. \end{aligned}$$

where E is the expectation operator.

The variance values can be estimated from knowledge of the error values of the accelerometer and voltmeter, as well as the errors associated with the discretization of the model.

Our goal is to estimate just the fractional differential equation coefficients. We will use generalized total least squares for this. The solving of generalized total least squares is reduced to finding the minimum of the objective function:

$$\min_{\theta} \frac{\|\tilde{\Phi}\theta - \tilde{\ddot{Z}} - g\|_2^2}{\sigma_{\xi}^2 + \theta^T W \theta}, \quad (13)$$

where

$$W = \begin{pmatrix} \sigma_{\xi}^2 & 0 \\ 0 & \sigma_{\zeta}^2 \end{pmatrix},$$

$\|\cdot\|_2$ is Euclidian norm,

W is the diagonal matrix of noise variances,

$$\sigma_{\xi}^2 = \frac{1}{N-1} \sum_{k=1}^N (\tilde{\ddot{z}}(t_k) - \ddot{z})^2, \tilde{\ddot{z}} = \frac{1}{N} \sum_{k=1}^N \ddot{z}(t_k).$$

The generalized total least squares problem (13) can be reduced to the total least squares problem

$$\min_{\theta_n} \frac{\|\tilde{\Phi}_n \theta_n - \tilde{\ddot{Z}} - g\|_2^2}{1 + \|\theta_n\|_2^2}, \quad (14)$$

where

$$\begin{aligned} \Phi_n^{(1)} &= \Phi^{(1)} \frac{\sigma_{\ddot{y}}}{\sigma_{\dot{y}}}, \Phi_n^{(2)} = \Phi^{(2)} \frac{\sigma_{\ddot{y}}}{\sigma_u}, \\ \theta_n^{(1)} &= \frac{\sigma_{\dot{y}}}{\sigma_{\ddot{y}}} \theta^{(1)}, \theta_n^{(2)} = \frac{\sigma_u}{\sigma_{\ddot{y}}} \theta^{(2)}. \end{aligned}$$

The minimum of objective function (14) can be found as a solution to the biased normal system of equations describe as

$$\hat{\theta}_n = (\Phi_n^T \Phi_n - \sigma^2 E)^{-1} \Phi_n^T (\ddot{Z} - g). \quad (15)$$

An augmented symmetric system of equations was used to calculate the total least squares (14) [Ivanov and Zhdanov, 2021b]

$$\begin{pmatrix} \sigma E_N & \Phi_n \\ \Phi_n^T & \sigma E_2 \end{pmatrix} \begin{pmatrix} \sigma^{-1} \varepsilon_n \\ \theta_n \end{pmatrix} = \begin{pmatrix} \ddot{Z} - g \\ 0 \end{pmatrix}, \quad (16)$$

where σ is minimal singular values of matrices $(\Phi_n, \ddot{Z} - g)$.

Perform inverse change of variable

$$\theta^{(1)} = \frac{\sigma_{\ddot{y}}}{\sigma_{\dot{y}}} \theta_n^{(1)}, \theta^{(2)} = \frac{\sigma_{\ddot{y}}}{\sigma_u} \theta_n^{(2)}.$$

5 Fractional Errors-in-Variables and Error in an Equation With Random Coefficients

A further generalization is a model that combines the error in the equation and errors in the variables:

$$\begin{aligned} \ddot{z}(t_k) - g &= \varphi(t_k)\theta + e(t_k), \tilde{z}(t_k) = \dot{z}(t_k) + \dot{\xi}(t_k), \\ \tilde{\ddot{z}}(t_k) &= \ddot{y}(t_k) + \ddot{\xi}(t_k), \tilde{u}(t_k) = u(t_k) + \xi_u(t_k). \end{aligned} \quad (17)$$

The assumption that noise sequences $\{\ddot{\xi}(t_k)\}, \{\dot{\xi}(t_k)\}$ are white noise is not always met. The article [Macias et al., 2022; Macias and Sierociuk, 2023] shows that the accelerometer error will be fractional white noise. Let us assume that

$$\tilde{z}(t_k) = \dot{z}(t_k) + \Delta^\alpha \dot{\xi}(t_k), \tilde{\tilde{z}}(t_k) = \ddot{z}(t_k) + \Delta^\beta \ddot{\xi}(t_k).$$

where

$$\Delta^\alpha \dot{\xi}(t_k) = \sum_{j=0}^i a_j \dot{\xi}(t_{k-j}),$$

$$\Delta^\beta \ddot{\xi}(t_k) = \sum_{j=0}^i b_j \ddot{\xi}(t_{k-j}),$$

$$a_j = \binom{\alpha_m}{j} = \frac{(-1)^j \Gamma(\alpha_m + 1)}{\Gamma(j+1)\Gamma(\alpha_m - j + 1)},$$

$$b_j = \binom{\beta_m}{j} = \frac{(-1)^j \Gamma(\beta_m + 1)}{\Gamma(j+1)\Gamma(\beta_m - j + 1)},$$

$$\Gamma(\alpha) = \int_0^\infty e^{-t} t^{\alpha-1} dt \text{ is the Euler's function.}$$

The error in the equation $\varsigma(t_k)$ may have a more complex parameterization such as a moving average, autoregression, etc. In general, the error model in the equation can be described as

$$e(t_k) = \frac{C(q^{-1})}{D(q^{-1})} \varsigma(t_k), \quad (18)$$

where

$$C(q^{-1}) = \sum_{j=0}^{n_c} c_j q^{-j}, D(q^{-1}) = \sum_{j=0}^{n_d} d_j q^{-j},$$

$q^{-1} \varsigma(t_k)$ is back shift operator, $\{\varsigma(t_k)\}$ is a white noise sequence.

Another important point is that the noise for the drone is non-stationary

$$e(t_k) = \frac{C(t_k, q^{-1})}{D(t_k, q^{-1})} \varsigma(t_k). \quad (19)$$

The noise model (19) can describe the following classes of random processes and not only [Marek, 2005]: linear ARMA models (18), time dependent ARMA models (The coefficients is not random, but it depends on t), self-exciting threshold moving average models, strongly subdiagonal bilinear models; ARCH models etc. Thus, the disturbance model for the drone:

$$\begin{aligned} \ddot{z}(t_k) - g &= \varphi(t_k) \theta + \frac{C(t_k, q^{-1})}{D(t_k, q^{-1})} \varsigma(t_k), \\ \tilde{\tilde{z}}(t_k) &= \ddot{z}(t_k) + \Delta^\beta \ddot{\xi}(t_k), \tilde{z}(t_k) = \dot{z}(t_k) + \Delta^\alpha \dot{\xi}(t_k), \\ \tilde{u}(t_k) &= u(t_k) + \xi_u(t_k). \end{aligned} \quad (20)$$

6 Extended Instrumental Variables and Generalized Instrumental Variables

The use of the generalized total least squares for estimation of vector requires knowledge of the samples of

the residual autocorrelation function. This task is very difficult to accomplish due to the non-stationary nature of disturbance (20). An alternative approach is instrumental variables [Söderström and Stoica, 1983]. The basic idea of instrumental variables is to select a vector that is correlated with the regression vector, but not correlated with the generalized error:

$$E(\psi(t_k) \varphi^T(t_k)) = H_{\psi\varphi}, E(\psi(t_k) \varepsilon(t_k)) = 0.$$

For problem (20), such a choice of instrumental variables can be described as [Söderström and Mahata., 2002]

$$\psi(t_k) = (\tilde{u}(t_{k-1}), \dots, \tilde{u}(t_{k-n}))^T. \quad (21)$$

To increase the accuracy of estimates, the dimension of the vector of instrumental variables is taken to be greater than the dimension of the regression vector

$$\dim(\psi(t_k)) > \dim(\varphi(t_k)). \quad (22)$$

Estimates can be found from solving the overdetermined system of equations:

$$\Psi^T \Phi \theta = \Psi^T (\tilde{Z} - g), \quad (23)$$

where

$$\Psi = \begin{pmatrix} \Psi(t_1) \\ \vdots \\ \Psi(t_N) \end{pmatrix}.$$

The LS solution of system of equations (20) is most often used:

$$\theta_{EIV} = \left((\Psi^T \Phi)^T \Psi^T \Phi \right)^{-1} (\Psi^T \Phi)^T \Psi^T (\tilde{Z} - g), \quad (24)$$

The augmented system equivalent to the normal system (24) is described as [Ivanov and Zhdanov, 2021a]

$$\begin{pmatrix} K_{EIV-LS} E_n & \Psi^T \Phi \\ \Psi \Phi^T & 0 \end{pmatrix} \begin{pmatrix} K_{EIV}^{-1} \varepsilon \\ \theta \end{pmatrix} = \begin{pmatrix} \Psi^T (\tilde{Z} - g) \\ 0 \end{pmatrix}, \quad (25)$$

where

$$K_{EIV-LS} = \frac{\sigma_{\min}(\Psi^T \Phi)}{\sqrt{2}}, \sigma_{\min}(\Psi^T \Phi) \text{ is minimal singular number of matrix } \Psi^T \Phi.$$

A TLS solution to the system of equations (23) is described as

$$\begin{aligned} \theta_{EIV-TLS} &= \left((\Psi^T \Phi)^T \Psi^T \Phi - \sigma_{EIV}^2 E \right)^{-1} \times \\ &\times (\Psi^T \Phi)^T \Psi^T (\tilde{Z} - g), \end{aligned} \quad (26)$$

The augmented system equivalent to the normal system (26) is described as [Ivanov and Zhdanov, 2021b]

$$\begin{pmatrix} \sigma_{EIV} E_n & \Psi^T \Phi \\ \Psi \Phi^T & \sigma_{EIV} E_2 \end{pmatrix} \begin{pmatrix} \varepsilon \\ \theta \end{pmatrix} = \begin{pmatrix} \Psi^T (\ddot{Z} - g) \\ 0 \end{pmatrix}, \quad (27)$$

where σ_{EIV} is minimal singular values of matrices $(\Psi^T \Phi, \Psi^T (\ddot{Z} - g))$.

Using a TLS solution is preferable to an LS solution on short samples [Ivanov, 2021; Ivanov et al., 2022]. The use of the instrumental variable with vector (21) can lead to ill conditionality of the matrix $(\Psi^T \Phi)^T \Psi^T \Phi$ or even incorrectness if input signal $u(t_k)$ it is white noise.

Generalized instrumental variables [Söderström, 2011; Ivanov et al., 2018] have better numerical stability. Let the vector of instrumental variables be partially correlated with the regression vector and have the form

$$\psi(t_k) = (\tilde{u}(t_k), \dots, \tilde{u}(t_{k-n}))^T, \quad (28)$$

Estimates of the vector of coefficients can be found from solving the overdetermined system of equations

$$(\Psi^T \Phi - \sigma_\zeta^2 H) \theta = \Psi^T (\ddot{Z} - g), \quad (29)$$

$$\text{where } H = \begin{pmatrix} 0 & 0 \\ 0 & 1 \\ \vdots & \vdots \\ 0 & 0 \end{pmatrix}.$$

Let us introduce the notation

$$X = \Psi^T \Phi - \sigma_\zeta^2 H,$$

then the LS solution of system (29) is described as

$$\theta_{GIV} = (X^T X)^{-1} X^T \Psi^T (\ddot{Z} - g). \quad (30)$$

The augmented system equivalent to the normal system (30) is described as [Björck, 1967]

$$\begin{pmatrix} K_{GIV-LS} E_n & X \\ X^T & 0 \end{pmatrix} \begin{pmatrix} K_{GIV-LS}^{-1} \varepsilon \\ \theta \end{pmatrix} = \begin{pmatrix} \Psi^T (\ddot{Z} - g) \\ 0 \end{pmatrix}, \quad (31)$$

where

$K_{GIV-LS} = \frac{\sigma_{\min}(X)}{\sqrt{2}}$, $\sigma_{\min}(X)$ is minimal singular number of matrix X .

A TLS solution to the system of equations (29) can also be found.

$$\theta_{GIV-TLS} = (X^T X - \sigma_{GIV}^2 E)^{-1} X^T \Psi^T (\ddot{Z} - g), \quad (32)$$

The augmented system equivalent to the normal system (32) is described as [Ivanov and Zhdanov, 2021b]

$$\begin{pmatrix} \sigma_{GIV} E_n & X \\ X^T & \sigma_{GIV} E_2 \end{pmatrix} \begin{pmatrix} \varepsilon \\ \theta \end{pmatrix} = \begin{pmatrix} \Psi^T (\ddot{Z} - g) \\ 0 \end{pmatrix}, \quad (33)$$

where σ_{GIV} is minimal singular values of matrix $(X, \Psi^T (\ddot{Z} - g))$.

7 Simulation Results

Thus, the disturbance model for the drone:

$$\begin{aligned} \ddot{y}(t_k) - g &= \varphi(t_k) \theta + \frac{(t_k, q^{-1})}{D(t_k, q^{-1})} \zeta(t_k), \\ \ddot{z}(t_k) &= \ddot{z}(t_k) + \Delta^{-0.5} \ddot{\xi}(t_k), \\ \dot{z}(t_k) &= \dot{z}(t_k) + \Delta^{-0.4} \dot{\xi}(t_k), \\ \tilde{u}(t_k) &= u(t_k) + \xi_u(t_k). \end{aligned} \quad (34)$$

where

$\theta = (0.293 \ 0.021)^T$,
 $\zeta(t_k) = c_1(t_k) e(t_{k-1}) + c_2(t_k) e(t_{k-2}) + \sin(0.01 t_k) + \sin(10 t_k)$,
 $\xi_{\dot{y}}(t_k)$, $\xi_{\dot{z}}(t_k)$, $\xi_u(t_k)$ are independent random variables with zero mean and constant variance;
 $c_1(t_k) \in N(0, 1)$, $c_2(t_k) \in N(3, 1)$ are Gaussian random variables.

The input signal is described as

$$u(t_k) = 0.7 \zeta_u(t_{k-1}) + 0.49 \zeta_u(t_{k-2}) + \sin(0.1 t_k^{1.1}), \quad (35)$$

where

$\zeta_u(t_k) \in N(0, 0.02)$ is Gaussian random variable.

Figure 2 shows values $u(t_k)$, $z(t_k)$.

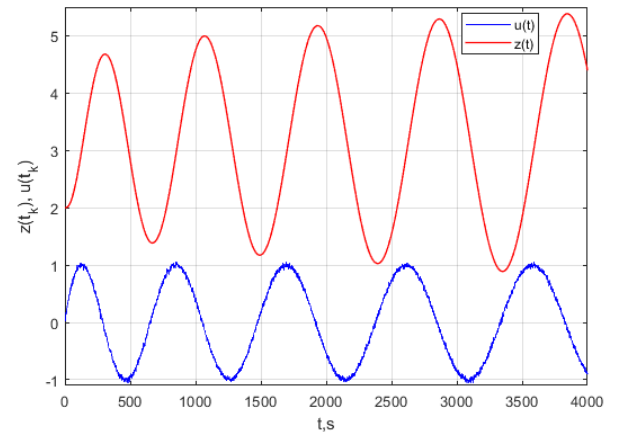


Figure 2. Values $u(t_k)$, $z(t_k)$.

The results are based on 100 independent Monte Carlo simulations. Sampling time $T_d = 0.2s$. The number of data points N in each simulation was 4000.

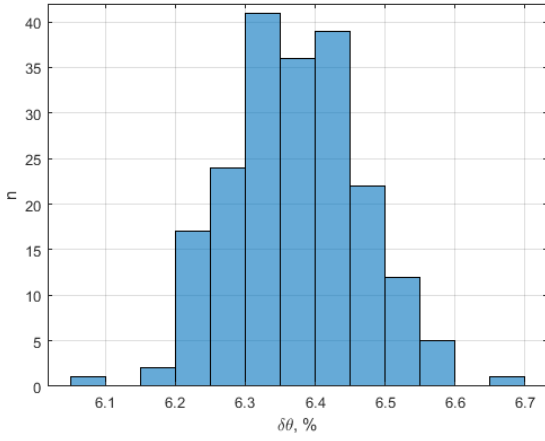


Figure 3. Histogram of NRMSE for LS

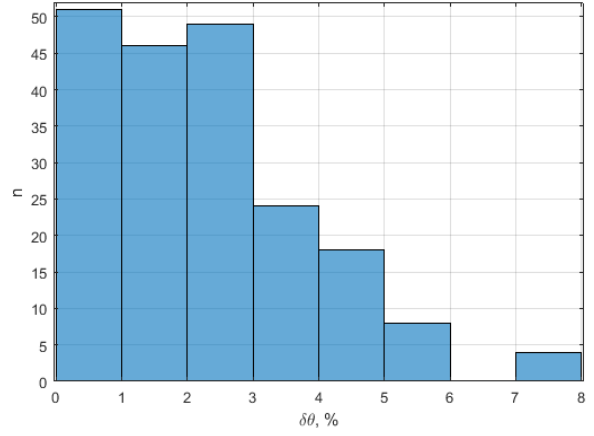


Figure 5. Histogram of NRMSE for GIV

Test examples were compared by the normalized root-mean-square error (NRMSE) of parameter estimation, defined as

$$\delta\theta_m = \sqrt{\frac{\|\hat{\theta}_m - \theta_m\|^2}{\|\theta_m\|^2}} \cdot 100\%, \delta\theta = \sqrt{\frac{\|\hat{\theta} - \theta\|^2}{\|\theta\|^2}} \cdot 100\%.$$

Example 1: Noise-to-signal ratio are $\sigma_{\xi u}/\sigma_u = \sigma_e/\sigma_{ij} = \sigma_{\xi ij}/\sigma_{ij} = 2 \cdot 10^{-3}, \sigma_{\xi ij}/\sigma_{ij} = 10^{-2}$.

For each method, we have given the sample mean and sample standard deviation denoted by SD.

Table 1. Mean and standard deviation of NRMSE

| | <i>LS</i> | <i>IV</i> | <i>GIV</i> |
|------------------|------------------|-------------------|-----------------|
| $\delta\theta_1$ | 6.43 ± 0.074 | 187.2 ± 119.4 | 2.30 ± 1.67 |
| $\delta\theta_2$ | 6.32 ± 0.075 | 129.3 ± 80.4 | 2.26 ± 1.65 |
| $\delta\theta$ | 6.42 ± 0.074 | 186.9 ± 119.2 | 2.30 ± 1.67 |

Figures 3-5 show histograms of NRMSE.

Example 2: Noise-to-signal ratio are $\sigma_{\xi u}/\sigma_u = \sigma_e/\sigma_{ij} = \sigma_{\xi ij}/\sigma_{ij} = 5 \cdot 10^{-3}, \sigma_{\xi ij}/\sigma_{ij} = 10^{-2}$.

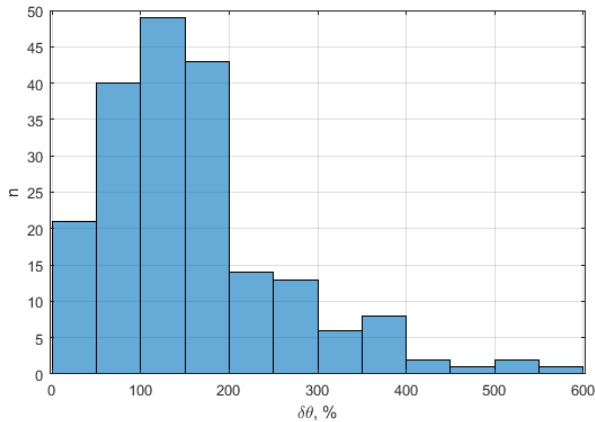


Figure 4. Histogram of NRMSE for EIV

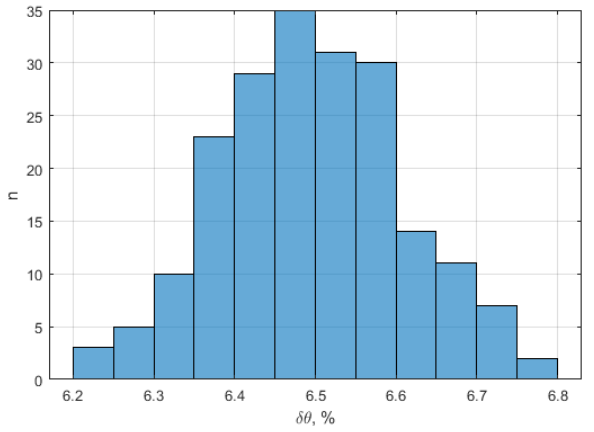


Figure 6. Histogram of NRMSE for LS

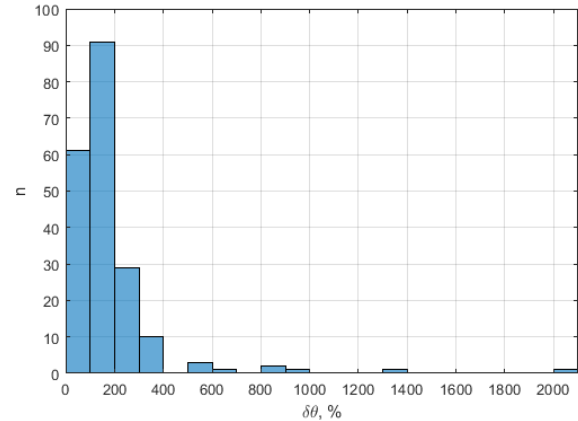


Figure 7. Histogram of NRMSE for EIV

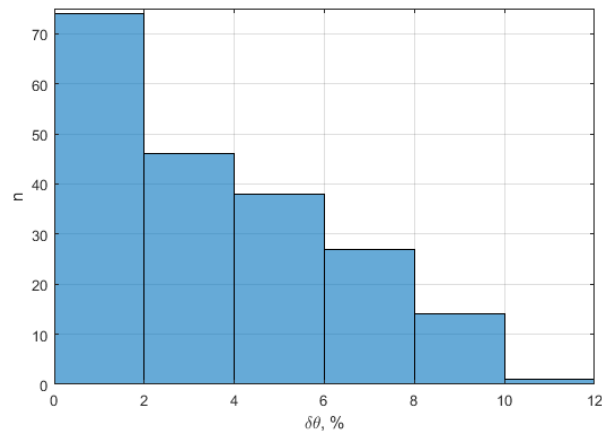


Figure 8. Histogram of NRMSE for GIV

For each method, we have given the sample mean and sample standard deviation denoted by SD.

Table 2. Mean and standard deviation of NRMSE

| | <i>LS</i> | <i>IV</i> | <i>GIV</i> |
|------------------|------------------|-------------------|------------------|
| $\delta\theta_1$ | 6.55 ± 0.10 | 211.6 ± 247.3 | 5.74 ± 2.70 |
| $\delta\theta_2$ | 6.442 ± 0.10 | 145.0 ± 159.7 | 3.69 ± 2.65 |
| $\delta\theta$ | 6.55 ± 0.10 | 211.6 ± 246.9 | 5.739 ± 2.70 |

Figures 6-8 show histograms of NRMSE.

8 Conclusion

The article proposes to consider the identification of a quadcopter vertical take-off model under conditions of non-stationary disturbances and observation interference in fractal white noise. It is proposed to use TLS to solve the problem of generalized instrumental variables. To improve numerical stability, a representation based on extended equivalent systems is proposed. Simulation results showed that the proposed approach allows more accurate LS and EIV.

On the other hand, LS has the smallest standard deviation. To further reduce the standard deviation of the estimation error, the development of a regularized version [Ivanov and Zhdanov, 2022] of generalized instrumental variables is an urgent task.

Acknowledgements

This article was supported by the Federal Agency of Railway Transport (No. 124040100033-0) and program for the development of the Scientific and Educational Mathematical Center of the Volga Federal District, Agreement No. 075-02-2024-1456.

References

Abas, N., Legowo, A., and Akmeliawati, R. (2011). Parameter identification of an autonomous quadrotor.

Proceeding of the 4th International Conference on Mechatronics (ICOM'11), pp. 1–8.

Amelin, K. (2012). Randomization in control for a small uav fly optimization under unknown arbitrary wind disturbances. *Cybernetics and Physics*, **1** (2), pp. 79–88.

Amelin, K., Andrievsky, B., and Tomashevich, S. (2019). Data exchange with adaptive coding between quadrotors in a formation. *Autom Remote Control*, **80**, pp. 150–163.

Amelin, K. and Maltsev, V. (2021). Using of the spsa method to improve the accuracy of the uav following a given route under the action of wind loads. *Cybernetics and Physics*, **10** (4), pp. 224–230.

Amelin, K., Tomashevich, S., and Andrievsky, B. (2015). Recursive identification of motion model parameters for ultralight uav. *IFAC-PapersOnLine*, **48** (11), pp. 233–237.

Avdeev, A., Assaleh, K., and Jaradat, M. A. (2021). Quadrotor attitude dynamics identification based on nonlinear autoregressive neural network with exogenous inputs. *Chin. J. Mech. Eng.*, **35** (4), pp. 265–289.

Belge, H. (2020). Estimation of small unmanned aerial vehicle lateral dynamic model with system identification approaches. *Balkan journal of electrical computer engineering*, **8** (2), pp. 121–126.

Bergamasco, M. (2014). Identification of linear models for the dynamics of a hovering quadrotor. *Automation and Remote Control*, **22** (5), pp. 1696–1707.

Björck, A. (1967). Iterative refinement of linear least squares solutions. *BIT Numer. Math.*, **7**, pp. 257–278.

Castillo, G., Lozano, R., and Dzul, A. (2005). *Modelling and Control of Mini-Flying Machines, Advances in Industrial Control*. Springer-Verlag.

Elgmili, N., Mjahed, M., Elkari, A., and Ayad, H. (2019). Quadrotor identification through the cooperative particle swarm optimization-cuckoo search approach. *Computational Intelligence and Neuroscience*, **2019**, pp. ID 8925165.

Gremillion, G. and Humbert, J. (2010). System identification of a quadrotor micro air vehicle. *Proc. of AIAA Conference on Atmospheric Flight Mechanics*, pp. 7644–7649.

Huang, J., Li, D., Wang, B., Zhang, Y., Mu, L., Jiao, S., and Liu, H. (2021). System parameter identification for a quadrotor uav by frequency domain method. *2021 China Automation Congress (CAC), Beijing, China*, pp. 1095–1100.

Ivanov, D. (2021). Identification ramsay curve total instrumental variables. *Lecture Notes in Networks and Systems*, **139**.

Ivanov, D., Granichin, O., O.Pankov, and O.Granichina (2023). Stabilizing -semioptimal fractional controller for discrete non-minimum phase system under unknown-but bounded disturbance. *Cybernetics and Physics*, **12** (2), pp. 121–128.

- Ivanov, D. and Zhdanov, A. (2021a). Numerically stable algorithm for identification of linear dynamical systems by extended instrumental variables. *J. Phys.: Conf. Ser.*, **1745**.
- Ivanov, D. and Zhdanov, A. (2021b). Symmetrical augmented system of equations for the parameter identification of discrete fractional systems by generalized total least squares. *Mathematics*, **9**.
- Ivanov, D. and Zhdanov, A. (2022). Implicit iterative algorithm for solving regularized total least squares problems. *Vestn. Samar. Gos. Tehnicheskogo Univ. Seriya Fiz.-Mat. Nauk.*, **26**(2), pp. 311–321.
- Ivanov, D. V., Sandler, I. L., and Kozlov, E. V. (2018). Identification of fractional linear dynamical systems with autocorrelated errors in variables by generalized instrumental variables. *IFAC-PapersOnLine*, **51**(32), pp. 580–584. 17th IFAC Workshop on Control Applications of Optimization CAO 2018.
- Ivanov, D. V., Sandler, I. L., Yakoub, Z., Antonova, V. V., Terekhin, M. A., and Bezyazykova, L. A. (2022). On instrumental variable-based method for identification of permanent magnet synchronous machine by noisy data. *2022 4th International Conference on Control Systems, Mathematical Modeling, Automation and Energy Efficiency (SUMMA)*, pp. 138–142.
- Janusz, W.C., C. R. and Szafranski, G. (2013). Identification and data fusion for the purpose of the altitude control of the vtol aerial robot. *2nd IFAC Workshop on Research, Education and Development of Unmanned Aerial Systems (RED-UAS 2013)*, pp. 263–269.
- Khaled, T. and Boumehraz, M. (2022). Black-box system identification for low-cost quadrotor attitude at hovering. *electrotehnica. Electrotehnica, Electronica, Automatica (EEA)*, **70**(4), pp. 88–97.
- Macias, M. and Sierociuk, D. (2023). Finite length triple estimation algorithm and its application to gyroscope mems noise identification. *Acta Mechanica et Automatica*, **17**.
- Macias, M., Sierociuk, D., and Malesza, W. (2022). Memes accelerometer noises analysis based on triple estimation fractional order algorithm. *Sensors*, **22**(2).
- Marek, T. (2005). On invertibility of a random coefficient moving average model. *Kybernetika*, **41**(6), pp. 743–756.
- Suliman, O., Heltha, I., Faliq, T., and Rahman, A. (2023). Dynamic modelling of drone systems using data-driven identification methods. *Lecture Notes in Electrical Engineering*, **882**.
- Söderström, T. (2011). A generalized instrumental variable estimation method for errors-in-variables identification problems. *Automatica*, **47**(8), pp. 1656–1666.
- Söderström, T. and Mahata, K. (2002). On instrumental variable and total least squares approaches for identification of noisy systems. *International Journal of Control*, **75**(6), pp. 381–389.
- Söderström, T. and Stoica, P. (1983). *Instrumental Variable Methods for System Identification*. Springer, Berlin.
- Wei, W., Schwartz, N., and Cohen, K. (2014). Frequency-domain system identification and simulation of a quadrotor controller. *Proc. of IAA Conference on Atmospheric Flight Mechanics*, pp. 1834–1839.
- Wei, W., Tischler, M., and Cohen, K. (2017). System identification and controller optimization of a quadrotor unmanned aerial vehicle in hover. *Journal of the American Helicopter Society*, **62**(4), pp. 1–9.
- Wu, M. and Lovera, M. (2019). Time-domain vs frequency-domain identification for a small-scale helicopter. *5th CEAS Specialist Conference on Guidance, Navigation and Control – EuroGNC*.
- Yang, S., Xi, L., Hao, J., and Wang, W. (2021). Aerodynamic-parameter identification and attitude control of quad-rotor model with cifer and adaptive ladrc. *Chin. J. Mech. Eng.*, **34**(1).